Attempt to determine the largest scale of primordial density perturbations in the universe

Arjun Berera
Department of Physics and Astronomy, Vanderbilt University, Nashville, Tennessee 37235

Li-Zhi Fang
Department of Physics, University of Arizona, Tucson, Arizona 85721

Gary Hinshaw
Laboratory for Astronomy and Solar Physics, Code 685, NASA/GSFC, Greenbelt, Maryland 20771
(Received 19 February 1997; published 23 January 1998)

The principle of causality requires that a pure power-law spectrum of cosmological density perturbations possess a super-Hubble suppression scale. We search for evidence of such suppression by performing a three parameter likelihood analysis of the COBE-DMR 4-year sky maps with respect to the amplitude, the spectral index, and the suppression scale. It is found that all suppression scales larger than c/H_0 are consistent with the data, but that scales of order c/H_0 are slightly preferred, at roughly the one-sigma level. Super-Hubble density fluctuations on very large scales ($\gg c/H_0$) can only be explained in the context of present theory by a de Sitter expansion phase, whereas those that are ''small'' ($\sim c/H_0$) can also be explained within the standard hot big-bang model. Density perturbations originating after any conceivable de Sitter expansion phase or during non-isentropic de Sitter expansion have natural kinematic constraints which could explain a small super-Hubble suppression scale. Standard inflationary cosmology, which is characterized by isentropic de Sitter expansion, generically predicts that the particle horizon should be much larger than the present-day Hubble radius, c/H_0. For such scenarios, a small super-Hubble suppression scale would require the duration of the inflation epoch to be fairly short. Suppression scales smaller than c/H_0 are strongly excluded by the COBE data. [S0556-2821(98)01106-0]

PACS number(s): 98.80.Es, 98.70.Vc, 98.80.Cq

I. INTRODUCTION

Causality prohibits coherence between physical phenomena with superhorizon scale separation. For density perturbations which are generated by local causal processes in a Robertson-Walker universe, the implications of causality have been shown to imply a suppression of the power spectrum which decreases faster than k^4 for scales larger than the horizon [1]. In non-inflationary cosmology the horizon and Hubble radius are about the same size, so that no causal mechanism could produce super-Hubble scale perturbations. Inflationary cosmology is characterized by a time period in which the horizon grew exponentially fast while the Hubble radius remained essentially constant. Thus inflation provides the only currently known causal mechanism that generates density perturbations on super-Hubble scales, greater than $c/H_0 \approx 3000\ \mathrm{h}^{-1}$ Mpc, where $\mathrm{h}^{-1} = 100/H_0$ km sec^{-1} Mpc^{-1}.

The power spectrum of the primordial scalar density perturbations can be written as

$$P(k) = A(ky)^n f(k), \tag{1}$$

where $y = 2c/H_0$ is the distance to the particle horizon in a matter dominated universe, and $f(k)$ is a function that describes the long wavelength suppression imposed by causality. Using very general arguments about causality, $f(k)$ can be obtained to have the form

$$f(k) = \frac{1}{1 + (k_{min}/k)^m}, \tag{2}$$

where k_{min} is the wave number of the suppression scale, and m is the suppression index. Causality places a strict constraint on the suppression index: $m \geq 4 - n$. A suppression factor like Eq. (2) also has been found in a model with cosmic strings plus cold or hot dark matter [2].

There is a second constraint on $f(k)$ imposed by causality, pertaining to the size of k_{min}, which may be useful in testing inflationary cosmology. Models of primordial density perturbations can be generally classified as either inflationary or non-inflationary, with the former type further classified as isentropic or non-isentropic. For all types of models, the long wavelength suppression of the spectrum is a general characteristic imposed by causality, although it is typically ignored in standard inflationary models. In non-inflationary models the causal horizon is about the same size as the present-day Hubble radius; thus causality implies the additional condition that $k_{min} \sim \pi H_0$ in these models. It should be noted that in non-inflationary models, density perturbations can be generated both prior to and after the epoch of last scattering, whereas Eq. (1) only strictly describes the former type. However, Eq. (1) may still apply to many types of perturbations generated after last scattering [3]. For both isentropic and non-isentropic inflationary models, k_{min} is far less constrained: In these models the largest density perturbations arose from the first fluctuations that crossed the Hubble radius during inflation [4]. The expansion factor for these per-

turbations is e^N, where N is the number of e-folds of growth in the cosmic scale factor. In order to solve the horizon problem, a key purpose of inflation, the minimum required expansion places a lower limit of $N \geqslant 50-70$. Standard inflationary models offer no convincing reason for N to be near its lower limit and generally predict it to be several orders of magnitude bigger. Hence the super-Hubble suppression scale in these models generally is expected to be large, $k_{min} \sim 0$. In the non-isentropic case, de Sitter expansion and radiation production are concurrent processes. In general, the interdependence of these two processes should place constraints on the overall expansion. In turn, restrictions on k_{min} are generally expected, but the specific form will depend on the details of the radiation production mechanism.

The power spectrum given by Eq. (1) contains four parameters: the amplitude A, the power-law spectral index n, the super-Hubble suppression scale wave number k_{min}, and the suppression index m. Previous analyses of the Cosmic Background Explorer (COBE) Differential Microwave Radiometer (DMR) maps have tacitly assumed that the suppression parameter k_{min} was zero. In this paper we perform a likelihood analysis of the DMR 4-year sky maps with respect to the first three parameters in Eq. (1). We fix the suppression index m at selected values and determine the most likely values of the amplitude A, the spectral index n, and the super-Hubble suppression scale k_{min}. From the results of this analysis, we place limits on the allowable range of k_{min}.

II. RADIATION SPECTRUM

In this analysis we consider the standard case of a flat universe with zero cosmological constant, $\Omega_0 = 1$ and $\Lambda = 0$. The cosmic microwave background radiation (CMB) temperature fluctuation in the direction $\hat{\mathbf{n}}$ is [5]

$$\frac{\delta T(\hat{\mathbf{n}})}{T} \equiv \frac{T(\hat{\mathbf{n}}) - T}{T} = -\frac{H_0^2}{2c^2 V^{1/2}} \sum_{\mathbf{k}} \frac{\delta(\mathbf{k})}{k^2} e^{-i\mathbf{k}\cdot\mathbf{y}}, \quad (3)$$

where $\delta(\mathbf{k})$ is the Fourier amplitude of the density contrast $\delta(\mathbf{r})$, $\mathbf{y}$ is a vector parallel to $\hat{\mathbf{n}}$ with length $y = 2c/H_0$, and V is a large volume (which cancels out in the final statistics). The power spectrum is defined as

$$P(k)\,\delta_{\mathbf{k}\mathbf{k}'} \equiv \langle \delta(\mathbf{k})\,\delta(\mathbf{k}') \rangle = \langle |\delta(\mathbf{k})|^2 \rangle \delta_{\mathbf{k}\mathbf{k}'}, \quad (4)$$

where the angular brackets denote ensemble average. $P(k)$ is assumed to have the form given in Eqs. (1) and (2).

Cosmic microwave background (CMB) temperature fluctuations may be expanded in spherical harmonics

$$\frac{\delta T(\hat{\mathbf{n}})}{T} = \sum_{lm} a_{lm} Y_{lm}(\hat{\mathbf{n}}), \quad (5)$$

where $Y_{lm}(\hat{\mathbf{n}})$ is a spherical harmonic function, and the a_{lm} are the expansion coefficients. Defining rotationally invariant coefficients $C_l \equiv 1/(2l+1) \Sigma_m \langle |a_{lm}|^2 \rangle$, and using Eq. (3), one finds

$$C_l = \frac{H_0^4}{2\pi c^4} \int_0^\infty dk \frac{P(k)}{k^2} |j_l(ky)|^2, \quad (6)$$

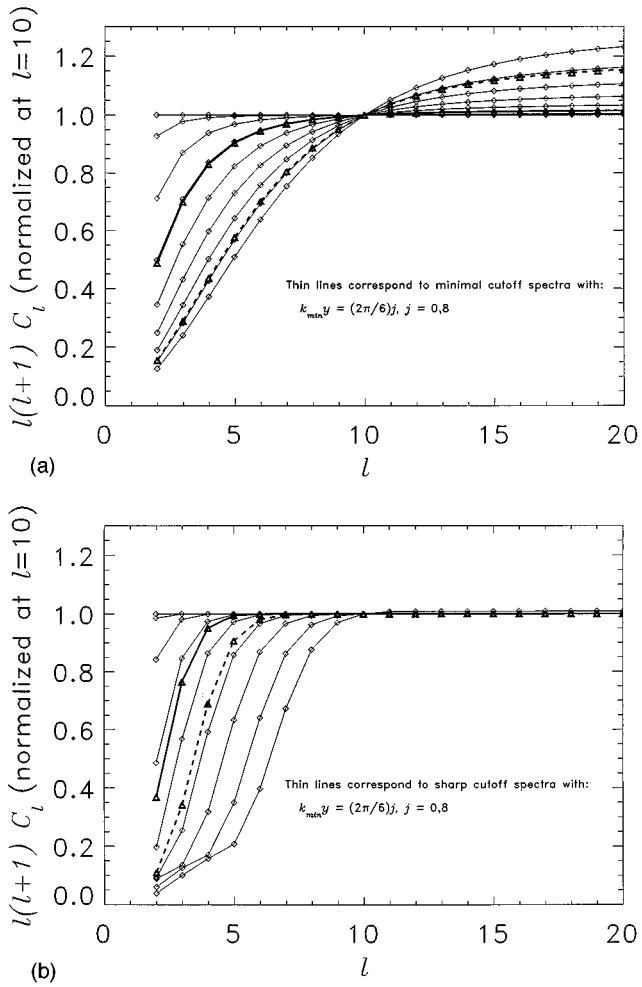

FIG. 1. C_l spectra for $n = 1$ and a range of $k_{min}y$ for (a) the minimal cutoff model and (b) the sharp cutoff model. The thin solid lines correspond to the values of $k_{min}y$ indicated in the panels. The thick solid line corresponds to the best fit $k_{min}y$; the thick dashed line corresponds to the 99% C.L. upper bound on $k_{min}y$. All spectra have been normalized to 1 at $l = 10$.

where $j_l(x)$ is the spherical Bessel function of order l. Using Eqs. (1) and (2), Eq. (6) becomes

$$C_l = \frac{AH_0^4}{2\pi c^4} \int_0^\infty \frac{dk}{k^2} \frac{(ky)^n |j_l(ky)|^2}{1 + (k_{min}/k)^m}. \quad (7)$$

With the above conventions, the quadrupole anisotropy is given by $Q_{rms\text{-}PS} = \sqrt{5C_2/4\pi}T$ where $T = 2.728$ K is the mean CMB temperature [6]. Plots of the C_l spectra with $n = 1$ for selected values of $k_{min}y$ are shown in Fig. 1. Note that the generic effect of a super-Hubble cutoff is to suppress the low order multipole moments.

To simplify the analysis, we have not considered temperature fluctuations produced by tensor (gravitational) perturbations. Most theoretical models predict the CMB anisotropy to be dominated by scalar perturbations. Tensor perturbation will be subject to a long wavelength suppression like Eq. (2), but the power spectrum index n will generally be different.

To check for possible confusion from secondary sources of anisotropy, such as the integrated Sachs-Wolfe (ISW) ef-

fect, we have generated fully processed power spectra with the code CMBFAST [7] for a range of the cosmological parameters Ω_{vac} and H, for which a significant ISW effect is possible. We find that the ISW effect generically increases the power in low-order multipoles and can thus ''fill in'' some of the suppression generated by causality. However, this requires values of Ω_{vac} in excess of ~ 0.5 to be significant, and in no case can the ISW effect *mimic* the effects of a small suppression scale. Thus we do not further consider the ISW effect in this paper since it cannot *decrease* the significance of any possible detection of a cutoff scale. Another possible source of confusion is due to Galactic emission: For example the quadrupole due to the Galaxy could partially cancel the quadrupole due to the CMB and suppress the overall quadrupole power. However, the studies performed to date suggest that this is not a significant effect [8].

The cutoff models, Eq. (7), have a mathematical similarity to the T^3-topology power spectrum models [9–12]. One can compare the spectra in Fig. 1 with Fig. 1 of [11]. This similarity is only a formal coincidence. These cutoff models in Eq. (7) are required in any causal theory and have no association with nontrivial topology.

III. METHOD

We use a pixel-based likelihood method to fit the parameters of our model power spectra. The method was pioneered in [13] and further used in DMR studies in [14,15]. This method is predated by Gaussian likelihood fits to the 2-point angular correlation function. The primary disadvantage of this approach is that the 2-point correlation function is not Gaussian distributed, and so a least squares fit is not necessarily a maximum likelihood fit.

In the pixel-based method we compute a likelihood function as follows. The probability of observing a map with pixel temperatures $\vec{T}$, given a model $C_l(\mathbf{p})$, where $\mathbf{p}$ denotes a set of parameters, is

$$P(\vec{T}|C_l(\mathbf{p}))d\vec{T}=\frac{d\vec{T}}{(2\pi)^{J/2}}\frac{e^{(-1/2)\vec{T}^T\cdot M^{-1}[C_l(\mathbf{p})]\cdot\vec{T}}}{\sqrt{\det M[C_l(\mathbf{p})]}} \tag{8}$$

where J is the number of pixels in the map, and M is the pixel-pixel covariance of the map (see below). Assuming a uniform prior distribution of model parameters, the probability (likelihood) of finding a given C_l, given a map $\vec{T}$, is then

$$L(C_l(\mathbf{p})|\vec{T})\propto\frac{e^{-(1/2)\vec{T}^T\cdot M^{-1}[C_l(\mathbf{p})]\cdot\vec{T}}}{\sqrt{\det M[C_l(\mathbf{p})]}}. \tag{9}$$

For convenience we will denote the likelihood function simply as $L(\mathbf{p})$.

The pixel-pixel covariance between pixels i and j is given by

$$M_{ij}\equiv\left\langle\frac{\delta T_i}{T}\frac{\delta T_j}{T}\right\rangle=\frac{1}{4\pi}\sum_l(2l+1)W_l^2C_lP_l(\hat{n}_i\cdot\hat{n}_j)+\sigma_i^2\delta_{ij}, \tag{10}$$

where δT_i is the temperature fluctuation in pixel i of the map, W_l^2 is the experimental window function that includes the effects of beam smoothing and finite pixel size, C_l is the power spectrum given in Eq. (7), $P_l(\hat{n}_i\cdot\hat{n}_j)$ is the Legendre polynomial of order l, $\hat{n}_i$ is the unit vector towards the center of pixel i, and σ_i is the rms noise expected in pixel i. If the pixel temperatures are Gaussian distributed, the covariance matrix fully specifies the statistics of the map.

We have evaluated the above likelihood function using the model power spectra in Eq. (7) for two cases: a sharp cutoff, $m=\infty$, and a minimal cutoff, $m=4-n$. The results reported below use the COBE ''correlation technique'' map which has an estimate of the high-latitude galaxy subtracted off [8]. We have also tested a case with a map that has no residual galaxy subtracted and find the results are not qualitatively different.

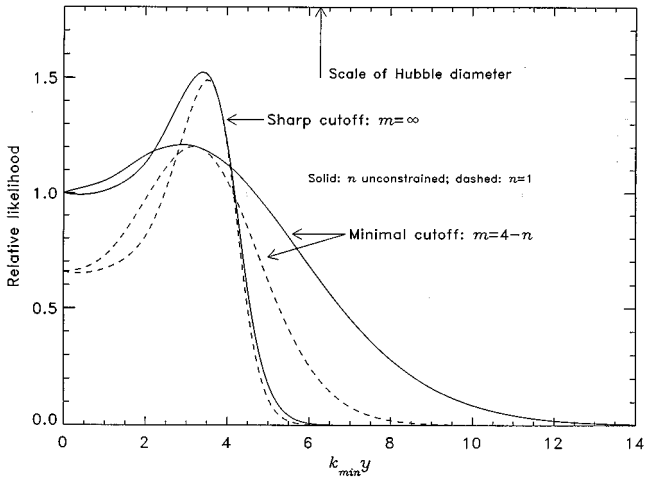

FIG. 2. Relative likelihood for the suppression scale wave number, k_{min}, projected over n and $Q_{rms\text{-}PS}$ with $y=2c/H_0$.

IV. RESULTS

The results of the analysis are presented in terms of projected likelihood functions: Given a set of parameters $\mathbf{p}=(\mathbf{p}_1,\mathbf{p}_2)$, the projected likelihood $L(\mathbf{p}_1;\mathbf{p}_2)$ is defined as $L(\mathbf{p})$ for fixed $\mathbf{p}_1$ evaluated at the most likely $\mathbf{p}_2$. In the following we define $Q\equiv Q_{rms\text{-}PS}$ for simplicity. A plot of the one-dimensional projected likelihood $L(k_{min};n,Q)$ is shown in Fig. 2. Contour plots of the two-dimensional projected likelihood $L(k_{min},n;Q)$ at 1, 2, and 3 sigma are shown in Figs. 3(a) and 3(b) for the minimal and sharp cutoff models respectively. Table I gives the most likely values of the three parameters obtained from the full likelihood. The uncertainties quoted in Table I are 68% confidence level (C.L.) and were obtained as follows. For k_{min} and n we projected the likelihood function to one dimension [$L(k_{min};n,Q)$ and $L(n;k_{min},Q)$ respectively] and integrated each function to obtain 68% confidence limits. For Q we sliced the likelihood at the most likely value of (k_{min},n) and integrated. The former procedure gives the uncertainty in a parameter with the other parameters unconstrained. The latter procedure gives the uncertainty in the normalization for a *fixed* spectral shape. Table II gives the most likely values of k_{min} and Q with the spectral index n fixed to 1. The uncertainties were obtained in the same manner as described above. Table III

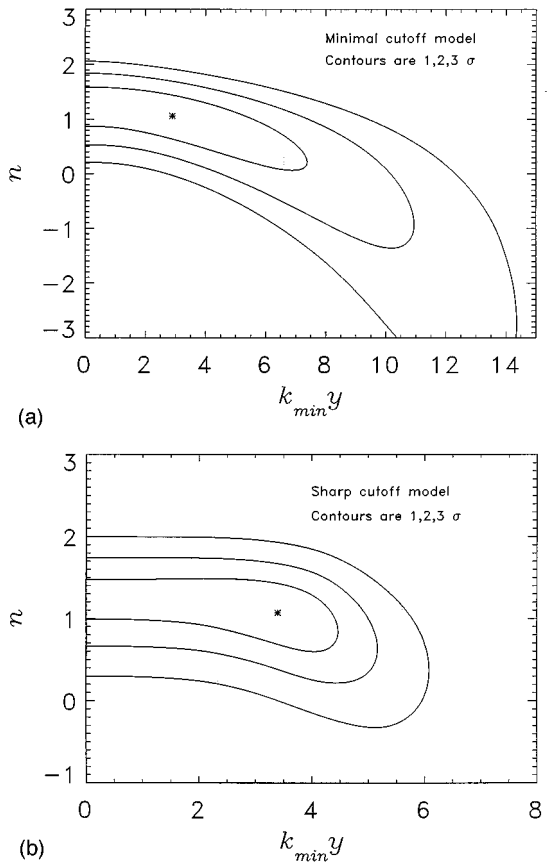

FIG. 3. Contour plots of $L(k_{min},n;Q)$ at 1, 2 and 3 sigma for (a) the minimal cutoff model and (b) the sharp cutoff model.

gives the 99% confidence upper limits on k_{min} for n unconstrained and for $n=1$. Our results reproduce those given in [15,16] in the limit $k_{min}=0$.

Table III supports a detection of a coherence length larger than the Hubble radius, c/H_0, for both cutoff models. Tables I and II show that all values of the suppression scale larger than the Hubble diameter ($\lambda_{Hubble}\sim 2c/H_0$) are consistent with the data, although scales of order $2\pi/k_{min}\approx 4c/H_0$ are slightly preferred. If the spectral index is fixed at $n=1$ (Table II), there is a one sigma exclusion of $k_{min}=0$. However, with n left unconstrained (Table I), only the sharp cutoff model is found to exclude $k_{min}=0$ at 68% confidence (Fig. 2). In no case was a two sigma exclusion of $k_{min}=0$ found.

Plots of the spectra, $l(l+1)C_l$, for $n=1$ are given in Figs. 1(a) and 1(b) for the minimal and sharp cutoff models, respectively. The thin solid lines show the spectra for a range of $k_{min}y$, the thick solid line corresponds to the most likely value of $k_{min}y$ (3.2 and 3.5 respectively) and the thick dashed line corresponds to the 99% C.L. upper bound on $k_{min}y$ (7.2 and 4.9 respectively). Note that a suppression of the low order multipole moments is a generic feature of power spectra that have a finite super-Hubble suppression scale.

It is instructive to compare the most likely spectra plotted in Fig. 1 with Fig. 3 of [17]. In that work the best fit power spectrum C_l was obtained from the 4-year DMR data by evaluating the likelihood with the C_l themselves as the free parameters. Ideally this is a model independent fit, although there were practical limitations to such an approach as discussed in the paper. The value of the quadrupole, C_2, found in [17] is similar to the value we find in the most likely cutoff power-law spectra. Similarly, our results for Q are consistent with those found in [15,16] where the quadrupole, C_2, was fit independent of the rest of the spectrum. This suggests that the shape of the likelihood in our current analysis is being driven primarily by the low quadrupole, and that the most likely spectra are such that the mean quadrupole in each case is comparable to the actual quadrupole in our sky. Note also that the most likely spectral index n is lower when k_{min} is simultaneously fit because the low quadrupole can be better fit with a non-zero k_{min} than with a steep spectrum, $n>1$.

The relative preference between the sharp and minimal forms of the cutoff can be measured by normalizing the likelihood at $k_{min}=0$, where both model spectra are common. By this measure the sharp cutoff is slightly preferred to the minimal cutoff—the ratio of the maxima of the two likelihood functions is 1.24.

To check the results of our likelihood analysis, we simulated 1000 pure power-law, scale-invariant sky maps, $(k_{min},n)=(0.0,1.0)$, to determine what fractions have likelihood functions similar to the data. The results of the Monte Carlo analysis are given in Table IV. For the upper limit on k_{min}, the Monte Carlo results confirm the 99% C.L. given in Table III for both types of cutoff. For the lower limit on k_{min}, the Monte Carlo results indicate that a pure power-law, scale invariant universe has a 20% (33%) chance of spuriously imitating a universe with a super-Hubble suppression scale of the size favored by the data given a sharp (minimal) cutoff. These results are consistent with the likelihood analysis. In particular, they verify that the suggestion found in the

TABLE I. Maximum likelihood parameter estimates with n unconstrained.

Super-Hubble cutoff	$k_{min}y$	n	$Q_{rms\text{-}PS}$ (μK)
Minimal ($m=4-n$)	$2.9^{+1.8}_{-2.9}$	$1.06^{+0.48}_{-0.67}$	13.0 ± 0.9
Sharp ($m=\infty$)	$3.4^{+0.7}_{-2.2}$	$1.07^{+0.32}_{-0.35}$	10.9 ± 0.7

TABLE II. Maximum likelihood parameter estimates with $n=1$.

Super-Hubble cutoff ($n=1$)	$k_{min}y$	$Q_{rms\text{-}PS}$ (μK)
Minimal ($m=4-n$)	$3.2^{+1.5}_{-2.0}$	12.8 ± 0.9
Sharp ($m=\infty$)	$3.5^{+0.8}_{-1.8}$	10.8 ± 0.7

TABLE III. 99% C.L. upper limits on $k_{min}y$.

Super-Hubble cutoff	$k_{min}y$	$k_{min}\vert_{(n=1)}$
Minimal ($m=4-n$)	10.5	7.2
Sharp ($m=\infty$)	5.0	4.9

TABLE IV. In columns 1 and 2, f is the fraction of simulated realization with k_{min} bigger than the most likely value found in the data, k_{data} for the minimal and sharp cutoff models. In column 3, f is the fraction of Monte Carlo simulated realizations with likelihood at $k=0$ less than that found in the data.

Super-Hubble cutoff	$f[k>k_{data}]$	$f[k(n=1)>k(n=1)_{data}]$	$f[L(k=0)<L(k=0)_{data}]$
Minimal ($m=4-n$)	334/1000	187/1000	314/1000
Sharp ($m=\infty$)	219/1000	156/1000	227/1000

data for a finite suppression scale *could* be due to spurious fluctuations about a pure power-law spectrum. The Monte Carlo results also indicate that increasing the signal-to-noise ratio with additional data could give perhaps 1–2 sigma greater discrimination of $k_{min}=0$, but cosmic variance prohibits much greater significance. In summary, a finite super-Hubble suppression scale is, at best, suggested by the data.

Finally, two features of the power spectrum model should be mentioned. First, for very large suppression scales, $k_{min}y<1$, the model spectra are virtually indistinguishable from a pure power-law spectrum. Hence this analysis is most powerful at placing upper limits on the suppression scale wave number k_{min}. Second, there is some degeneracy between k_{min} and n, particularly for the minimal form of the cutoff with $m=4-n$: Decreasing the suppression scale $2\pi/k_{min}$ partially mimics a steeper slope (larger n) in the power spectrum at low spherical harmonic order l. Additional large and medium scale anisotropy data, as expected from the forthcoming satellites Microwave Anisotropy Probe (MAP) and PLANCK, should allow us to place better limits on n so as to partly constrain this degeneracy.

V. DISCUSSION

This analysis establishes a firm lower limit on the suppression length scale of density perturbations and slightly favors a finite super-Hubble suppression scale. The standard assumption of a pure power-law primordial spectrum is equivalent to assuming an infinite suppression length scale, $k_{min}=0$. Almost any theoretical model of density perturbations has an implied suppression scale. Below we elucidate the suppression scales expected in various models. The standard inflationary models predict $k_{min}\sim 0$, which is consistent with, but not preferred by, the data. It is worth noting that the super-Hubble suppression behavior in the basic new inflation [18] and in chaotic inflation [19] is closer to the sharp cutoff form. For a large class of non-inflationary models there is no mechanism for the growth of super-Hubble scale perturbations. In models with a ''late time '' cosmological phase transition [20], we expect $k_{min}y\geqslant 4$ [1,3]. In models with topological defects, in which the perturbations are produced before last scattering, the super-Hubble suppression scale depends on the dynamics of the defects. For example, in models with cosmic strings plus hot or cold dark matter it was found that $k_{min}y\sim 2.1$–7.9 with a cutoff behavior closer to the minimal form [2]. These two types of non-inflationary models are potentially consistent with the COBE data, but subhorizon evolution must be checked. For cosmic strings, recent simulations [21] indicate that subhorizon evolution induces greater power in the low-order multipoles, C_{ℓ}. If further study supports this finding, it might be difficult to reconcile with the small quadrupole seen in the COBE data. Both the super-Hubble suppression scale and the form of the cutoff should be noted in all theoretical models of primordial density perturbations.

If the suggestion of a small super-Hubble suppression length scale is later substantiated, there are at least three possible explanations. One is that density perturbations produced by non-inflationary models are the dominant source. The second is that density perturbations are produced during an isentropic de Sitter expansion phase, which is synonymous with standard inflation. The third is that perturbations are produced during a non-isentropic de Sitter expansion phase. For either of these latter two cases, the number of e-folds, N, would have to be close to its lower bound. Such an interpretation could also explain a nearly flat to open universe [22]. In standard inflationary models a small N is viewed as a fine-tuning of the theory. The regime of non-isentropic de Sitter expansion may be further divided, depending on whether the radiation energy density decreases monotonically or requires a sharp increase during the transition back to the radiation dominated era. The former possibility was considered in [23], where it was shown in the context of standard Friedmann cosmology that a small N can be naturally realized by a symmetry breaking phase transition at finite temperature, during which the universe smoothly goes from an inflation-like stage to a radiation dominated stage without an intermediate period of reheating. The naturalness of a small N found in [23] motivated the search in this paper for a finite super-Hubble suppression scale. The non-isentropic, inflation-like expansion regime in [23] avoids (a) localized fields on ultra flat potential surfaces and (b) an impulsive, large-scale energy release during a reheating period [4]. The latter event must be isotropic over vastly disconnected causal regions. Both of these conundrums have been difficult to resolve in the standard inflationary picture. The theory of density perturbations in this intermediate regime of radiation and vacuum energy [24] requires further study of warm inflation [25] and other possible mechanisms before direct comparison is possible with standard inflationary models.

VI. CONCLUSION

The super-Hubble suppression scale added to the power spectrum in this paper is required on first principles by any causal theory. It is more fundamental than the spectral index and the amplitude and much less model dependent than other

processes that can effect the large-scale anisotropy, such as the integrated Sachs-Wolfe effect. Moreover, the suppressing effect of causality on the power spectrum can produce a potentially significant effect on large scales that is not readily confused with other processes that generically boost the large-scale anisotropy power.

In conclusion, we have modified the primordial power spectrum of density perturbations from a pure power-law form to a form that includes a super-Hubble suppression scale, k_{min}, so as to properly respect causality constraints. We fit this spectrum to the 4-year COBE-DMR sky maps and find that the data prefer a finite suppression scale, but do not rule out $k_{min}=0$. The best fit to the data is $(k_{min}y, n, Q_{rms\text{-}PS}) = (3.4^{+0.7}_{-2.2}, 1.07^{+0.32}_{-0.35}, 10.9 \pm 0.7\ \mu\mathrm{K})$, with a slight preference for a sharp form of the cutoff. Upper limits on $k_{min}y$ have been firmly established for the two limiting forms of the cutoff. We conclude that the fundamental parameter k_{min} can be identified in COBE-DMR data.

ACKNOWLEDGMENTS

Financial support was provided in part by the U.S. Department of Energy and the NASA Office of Space Sciences.

[1] L. F. Abbott and J. Traschen, Astrophys. J. **302**, 39 (1986); J. Robinson and B. D. Wandelt, Phys. Rev. D **53**, 618 (1996).
[2] A. Albrecht and A. Stebbins, Phys. Rev. Lett. **68**, 2121 (1992); **69**, 2615 (1992).
[3] A. H. Jaffe, A. Stebbins, and J. A. Frieman, Astrophys. J. **420**, 9 (1994).
[4] E. W. Kolb and M. S. Turner, *The Early Universe* (Addison-Wesley, New York, 1990).
[5] P. J. E. Peebles, Astrophys. J. Lett. **263**, L1 (1982).
[6] D. J. Fixsen *et al.*, Astrophys. J. **473**, 576 (1996).
[7] U. Seljak and M. Zaldarriaga, Astrophys. J. **469**, 437 (1996).
[8] A. Kogut *et al.*, Astrophys. J. Lett. **464**, L5 (1996).
[9] G. F. R. Ellis, Gen. Relativ. Gravit. **2**, 7 (1971).
[10] Y. P. Jing and L. Z. Fang, Phys. Rev. Lett. **73**, 1882 (1994).
[11] A. De Oliveira-Costa and G. F. Smoot, Astrophys. J. **448**, 477 (1995).
[12] A. De Oliveira-Costa, G. F. Smoot, and A. A. Starobinsky, Astrophys. J. **468**, 457 (1996).
[13] J. R. Bond, Phys. Rev. Lett. **74**, 4369 (1995).
[14] M. Tegmark and E. F. Bunn, Astrophys. J. **455**, 1 (1995).
[15] G. Hinshaw *et al.*, Astrophys. J. Lett. **464**, L17 (1996).
[16] C. L. Bennett *et al.*, Astrophys. J. Lett. **464**, L1 (1996).
[17] K. M. Górski, presented at 31st Rencontres de Moriod, 1996, astro-ph/9701191.
[18] J. M. Bardeen, P. J. Steinhardt, and M. S. Turner, Phys. Rev. D **28**, 679 (1983).
[19] A. Linde, Phys. Lett. **129B**, 177 (1983).
[20] I. Wasserman, Phys. Rev. Lett. **57**, 2234 (1986); W. H. Press, B. Ryden, and D. Spergel, *ibid.* **64**, 1084 (1990); G. Fuller and D. N. Schramm, Phys. Rev. D **45**, 2595 (1992); J. A. Frieman, C. T. Hill, and R. Watkins, *ibid.* **46**, 1226 (1992).
[21] B. Allen *et al.*, Phys. Rev. Lett. **77**, 3061 (1997).
[22] G. F. R. Ellis, Class. Quantum Grav. **5**, 891 (1988).
[23] A. Berera, Phys. Rev. D **55**, 3346 (1997).
[24] A. Berera and L. Z. Fang, Phys. Rev. Lett. **74**, 1912 (1995).
[25] A. Berera, Phys. Rev. Lett. **75**, 3218 (1995); Phys. Rev. D **54**, 2519 (1996).